NREL
NATIONAL RENEWABLE ENERGY LABORATORY

Outdoor PV Module Degradation of Current-Voltage Parameters

Preprint

Ryan M. Smith, Dirk C. Jordan,
and Sarah R. Kurtz

To be presented at the 2012 World Renewable Energy Forum
Denver, Colorado
May 13–17, 2012

Conference Paper
NREL/CP-5200-53713
April 2012

Contract No. DE-AC36-08GO28308

Available electronically at http://www.osti.gov/bridge

Available for a processing fee to U.S. Department of Energy
and its contractors, in paper, from:

U.S. Department of Energy
Office of Scientific and Technical Information
P.O. Box 62
Oak Ridge, TN 37831-0062
phone: 865.576.8401
fax: 865.576.5728
email: mailto:reports@adonis.osti.gov

Available for sale to the public, in paper, from:

U.S. Department of Commerce
National Technical Information Service
5285 Port Royal Road
Springfield, VA 22161
phone: 800.553.6847
fax: 703.605.6900
email: orders@ntis.fedworld.gov
online ordering: http://www.ntis.gov/help/ordermethods.aspx

Cover Photos: (left to right) PIX 16416, PIX 17423, PIX 16560, PIX 17613, PIX 17436, PIX 17721

Printed on paper containing at least 50% wastepaper, including 10% post consumer waste.

OUTDOOR PV MODULE DEGRADATION OF CURRENT-VOLTAGE PARAMETERS

Ryan M. Smith
Dirk C. Jordan
Sarah R. Kurtz
National Renewable Energy Laboratory
1617 Cole Boulevard
Golden, CO 80401
email: ryan.smith@nrel.gov

ABSTRACT

Photovoltaic (PV) module degradation rate analysis quantifies the loss of PV power output over time and is useful for estimating the impact of degradation on the cost of energy. An understanding of the degradation of all current-voltage (I-V) parameters helps to determine the cause of the degradation and also gives useful information for the design of the system. This study reports on data collected from 12 distinct mono- and poly-crystalline modules deployed at the National Renewable Energy Laboratory (NREL) in Golden, Colorado. Most modules investigated showed < 0.5%/year decrease in maximum power due to short-circuit current decline.

1. INTRODUCTION

Long-term performance of photovoltaic (PV) systems is vital to their continuing success in the market place. The gradual energy output loss over long periods of time is a major concern to all renewable energy stakeholders. A wide variety of degradation rates has been reported in the literature with respect to technologies, age, manufacturers, and geographic locations, and has been recently summarized. [1] Significant variation in the data can be caused by different module types, age, construction (encapsulation, front- and back-sheet), electrical set-up (open-circuit, short-circuit, load resistor, grid-tied), and measurement uncertainty. [2] The literature contains an excellent review of long-term field testing based on discreet I-V measurements [3], but fewer reports include more comprehensive I-V parameters investigation, including voltage and current at maximum power point. [4, 5, 6] In this paper we present results of detailed I-V measurements on 12 crystalline silicon (Si) modules located at the National Renewable Energy Laboratory (NREL) in Golden, Colorado.

2. EXPERIMENTAL DETAILS

Over the past 17 years, 100 modules have been installed on the Performance and Energy Ratings Testbed (PERT) at NREL's Outdoor Test Facility (OTF). Module installation dates vary greatly, with the earliest installation in 1993. There is an equally large variation in the monitoring times, from merely a few months to more than 17 years of continuous data. The modules, mounted side-by-side at the latitude tilt of 40º (±1°) facing south (±2°), were held at maximum power with current-voltage curves taken typically every 15 minutes. Environmental parameters were recorded simultaneously and included plane-of-array (POA) irradiance (W/m^2), wind speed (m/s), ambient temperature (°C), and back-of-module temperature (°C). To date over 6.2 million I-V curves have been captured, with some of the earliest modules characterized by over 194,000 curves. Further details are discussed elsewhere. [7]

Fig. 1: Performance and Energy Ratings Testbed (PERT) at NREL. Photo credit: Warren Gretz, NREL PIX 03877.

3. MODELING CRITICAL I-V PARAMETERS

Determining degradation rates accurately for individual I-V parameters, such as short-circuit current (I_{sc}), open-circuit voltage (V_{oc}), maximum power (P_{max}), maximum current (I_{max}), maximum voltage (V_{max}), and fill factor (FF), required extraction of these parameters from each I-V curve. The manufacturer of the I-V curve tracer generates these values internal to the device, but the method is not robust for all data sets, so additional modeling was completed. Each I-V curve was composed of up to 300 discrete current and voltage pairs and due to incomplete scans or other anomalies, extraction of the six parameters varies with the extraction technique.

Fig. 2 shows modeled compared to measured values for FF, I_{max}, I_{sc}, P_{max}, V_{max}, and V_{oc} as a percentage of the maximum measured value. Significant discrepancies necessitated the modeling and may have a variety of causes. For instance, sometimes the I-V sweep was incomplete, leading to erroneous values. Another source of error was particularly on variable days when the POA irradiance changed significantly during the I-V sweep; many of these sweeps were excluded from analysis. Further examples are illustrated in Fig. 3 that show the measured curve and the modeled sections. Particularly the ends of the I-V curve were not always captured correctly, as is illustrated in inset (a). Inset (b) demonstrates a situation in which the modeled P_{max} point falls between the discrete points. Modeling of these critical points required dividing the measurement points into smaller sets representing the conditions near I_{sc}, P_{max}, and V_{oc}. The method used to isolate the measurement points for modeling was based on the ASTM standard E1036-08, sections 8.5 through 8.10. [8] I_{sc} and V_{oc} were obtained by extrapolating using linear fits. As an addition to E1036-08, a minimum of six unique current-voltage pairs were required. The points near the expected P_{max} were modeled using a 4th order polynomial fit and the maximum point determined from the first derivative. [9]

Subsequently, I_{max} and V_{max} were obtained and the FF was calculated using the extrapolated values obtained for V_{oc} and I_{sc}.

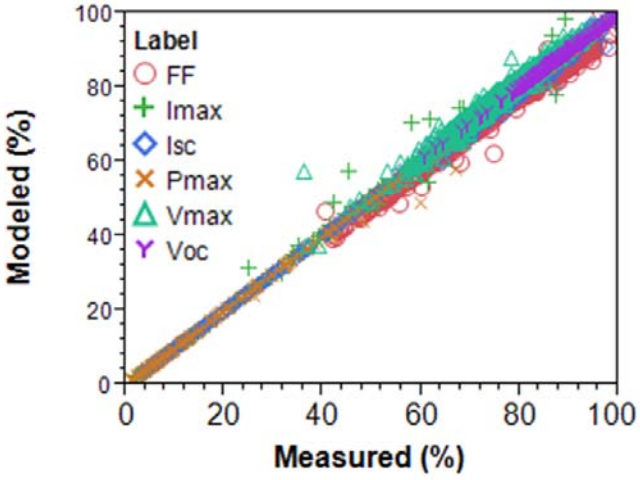

Fig. 2: Modeled versus measured I-V parameters as a percentage of the maximum measured value.

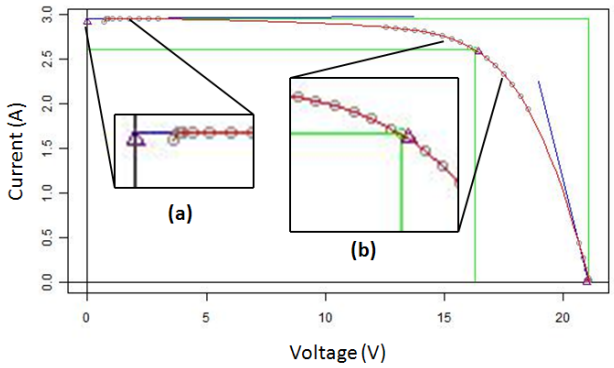

Fig. 3: Typical I-V curve showing measured and modeled parts of the curve. Insets (a) and (b) illustrate examples of issues that can lead to discrepancies between measured and modeled values.

4. DEGRADATION RATE DETERMINATION

Module temperature coefficients for I_{sc}, V_{oc}, and P_{max} (α, β, and γ, respectively) were determined from the measured data by filtering to a specific set of environmental conditions with considerations made to the requirements of IEC 61215 edition 2, section 10.4 for the determination of temperature coefficients. First, a narrow band of measurements captured between 980 and 1020 W/m^2 POA irradiance were included. The ±20 W/m^2 range around the standard test conditions (STC) [10] irradiance was chosen, as it provided a reasonable compromise between stability in the calculated temperature coefficients, low calculated uncertainty in the derived temperature coefficients, and an acceptable number of points from which the coefficients were determined.

When the filtering interval was further reduced, the uncertainty increased significantly due to the reduced number of data points and their disproportional influence.

Second, the difference between pre- and post-trace POA irradiance measurements was restricted to < 8 W/m^2 in order to reduce the impact of irradiance changes on the shape of the captured I-V curve. This interval appeared to be a good compromise between a narrow filter and its dramatically reduced number of available curves and a wider filter with an increase in the number of distorted curves. Note that IEC 61215 edition 2, section 10.4 requires that irradiance be limited to ±2% (±20 W/m^2) to eliminate variable conditions; this is more than double the range used in this study.

Finally, the ambient temperature and the difference between the ambient and module backsheet temperature were restricted to >10°C to eliminate traces when modules were fully or partially covered with snow. A linear fit of modeled V_{oc}, modeled I_{sc}, and modeled P_{max} to module temperature provided an intercept and a slope for each parameter from which the relative thermal coefficients were calculated at a reference module temperature of 45ºC, a realistic operating point for the climate.

Figures 4 through 6 detail the empirically derived relative temperature coefficients for the modules covered in this study and compare them to temperature coefficients tabulated from over 280 manufacturer data sheets of these technologies. It was noted that the determination of β and γ from outdoor current-voltage data was more accurate than the determination of α due to the high degree of linearity of V_{oc} and P_{max} to module temperature. The temperature coefficients derived from outdoor data correspond well with those published by the manufacturers, who most likely state the values determined through IEC 61215 qualification testing for terrestrial crystalline silicon modules.

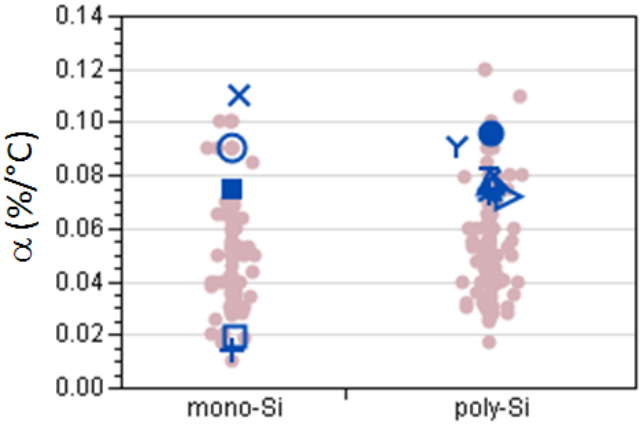

Fig. 4: Relative temperature coefficients of current, α, by technology. Blue symbols represent the coefficients calculated from field data. Faded solid circles represent coefficient values from manufacturer data sheets. For better visibility, the data were jittered in the x-axis.

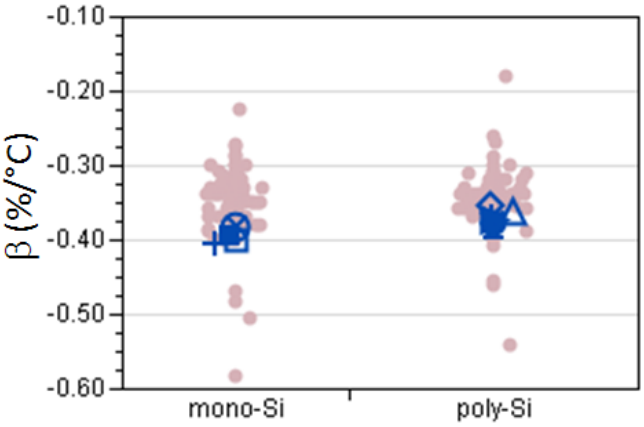

Fig. 5: Relative temperature coefficients of voltage, β, by technology. Blue symbols represent the coefficients calculated from field data. Faded solid circles represent coefficient values from manufacturer data sheets.

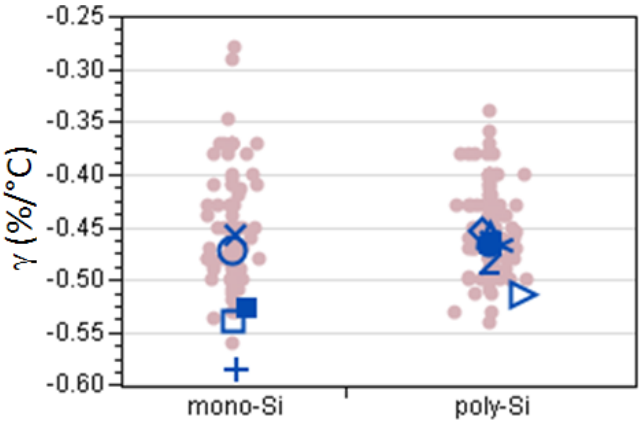

Fig. 6: Relative temperature coefficients of maximum power, γ, by technology. Blue symbols represent the coefficients calculated from field data. Faded solid circles represent coefficient values from manufacturer data sheets.

The number of manufacturers expressing uncertainties in the temperature coefficients was limited. Of over 280 data sheets tabulated for comparison, only 10 stated uncertainties in their temperature coefficients. Of interest to our work is the observation that the manufacturer-stated uncertainties of α, β, and γ are, on average, 26%, 8.5%, and 9.6% of the coefficient magnitude, respectively. The calculated uncertainties for the coefficients derived from field data are 9.6%, 1.1%, and 1.3%, respectively.

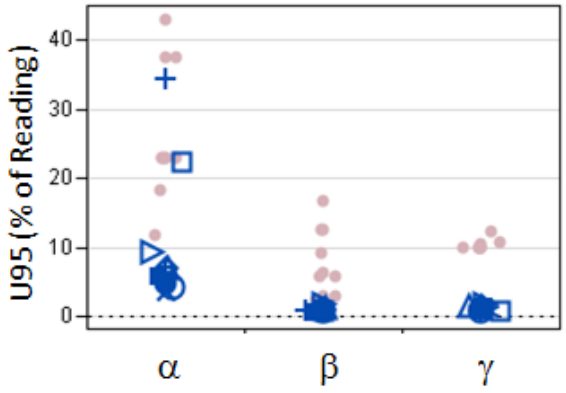

Fig. 7: Uncertainty of manufacturer's' temperature coefficients (faded solid circles) and calculated module temperature coefficients (blue symbols).

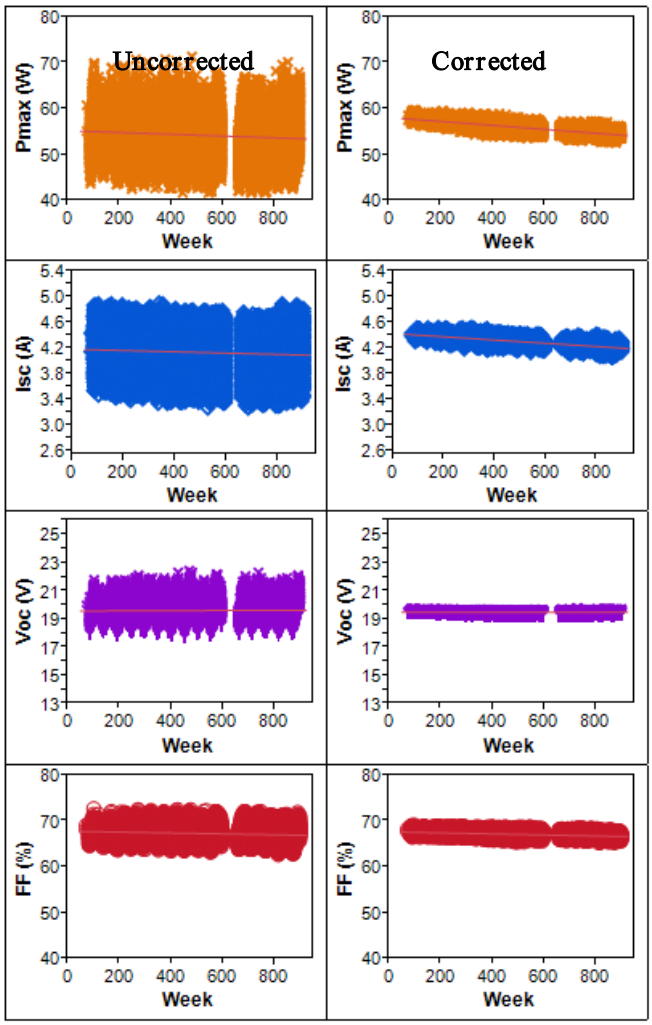

Fig. 8: Uncorrected (left) and irradiance- and temperature-corrected values (right) for P_{max}, I_{sc}, V_{oc}, and FF, respectively.

Degradation rates were calculated from a reduced data set established using parameter filters: 800 to 1100 W/m^2 POA irradiance and < 8W/m^2 pre- to post-trace POA irradiance delta. Correction of each critical I-V curve parameter was performed using well-established methods and reproduced in equations (1) through (6). [11, 12] The open-circuit voltage calculation was simplified to exclude δ(T), the V_{oc} correction for irradiance as a function of temperature. This simplification has a small effect on the absolute values that are reported, but a negligible effect on the measured degradation rates. In these equations, G is the POA irradiance (W/m^2) and T is the module temperature (ºC).

Corrected conditions consist of POA of 1000 W/m^2 and a more normal operating condition of 45ºC, rather than the STC condition of 25ºC, and are indicated by the zero subscripts.

TABLE 1: DEGRADATION RATE SUMMARY

Module	Manufacturer	Technology	$R_d P_{max}$	$R_d I_{sc}$	$R_d V_{oc}$	$R_d FF$	$R_d I_{max}$	$R_d V_{max}$	Years
1	A	mono	-0.29	-0.19	-0.02	-0.08	-0.20	-0.11	9.3
2	A	mono	-0.33	-0.27	-0.01	-0.06	-0.30	-0.08	8.1
3	A	mono	-0.21	-0.21	-0.03	0.03	-0.16	-0.07	9.3
4	A	mono	-0.25	-0.10	-0.02	-0.14	-0.25	-0.02	9.4
5	B	poly	-0.04	-0.14	-0.02	0.13	-0.04	0.03	10.4
6	B	poly	-0.07	-0.15	0.01	0.07	-0.16	0.12	10.4
7	C	mono	-0.39	-0.30	-0.01	-0.09	-0.30	-0.06	17.2
8	D	poly	0.29	0.24	0.05	0.00	0.25	0.08	6.4
9	D	poly	-0.07	0.16	0.02	-0.24	-0.10	0.10	6.4
10	D	poly	-0.85	-0.23	-0.07	-0.58	-0.65	0.02	3.8
11	E	poly	-1.14	-0.24	0.00	-0.96	-0.46	-0.76	11.6
12	E	poly	-0.61	-0.26	-0.06	-0.33	-0.30	-0.30	12.7
Median			-0.27	-0.20	-0.01	-0.08	-0.23	-0.04	9.4
St Dev			0.38	0.17	0.03	0.31	0.22	0.24	3.4

$$I_{SC_0} = \left(\frac{G_0}{G}\right)\left[\frac{I_{SC}}{1+\alpha(T-T_0)}\right] \quad (1)$$

$$V_{OC_0} = \left[\frac{V_{OC}}{1+\beta(T-T_0)}\right] \quad (2)$$

$$P_{max_0} = \left(\frac{G_0}{G}\right)\left[\frac{P_{max}}{1+\gamma(T-T_0)}\right] \quad (3)$$

$$I_{max_0} = \frac{I_{max}\left(\frac{G_0}{G}\right)}{(1+\alpha(T-T_0))} = I_{max}\left(\frac{I_{SC_0}}{I_{SC}}\right) \quad (4)$$

$$V_{max_0} = \frac{V_{max}}{1+\beta(T-T_0)} = V_{max}\left(\frac{V_{OC_0}}{V_{OC}}\right) \quad (5)$$

$$FF_0 = \left[\frac{P_{max_0}}{I_{SC_0} V_{OC_0}}\right] \quad (6)$$

In the first step, the filtered data were grouped into blocks representing one week of measurements, and the mean value for each parameter block was calculated. Second, the weekly averaged data are graphed as a time series and degradation rates are determined from a linear least-squares fit. Fig. 8 shows uncorrected (left) and irradiance- and temperature-corrected values (right) for P_{max}, I_{sc}, V_{oc}, and FF, respectively. The statistical uncertainty for the degradation rate is a Type A uncertainty according to the ISO Guide to the Expression of Uncertainty and can be calculated directly from the standard errors of the regression and using error propagation. [13] This process was repeated for the 12 modules in this study, the results of which are summarized in Figures 9 and 10 and Table 1. All degradation rates in Table 1 are in (%/year).

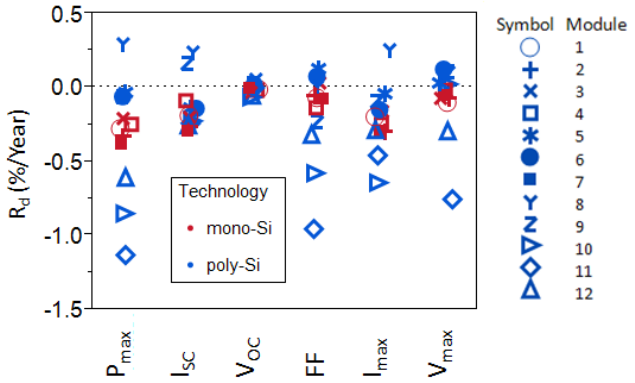

Fig. 9: Degradation rates for individual I-V parameters. Each module is represented by a different symbol. Mono-Si are in red while poly-Si modules are in blue. A negative value implies decreased performance with time.

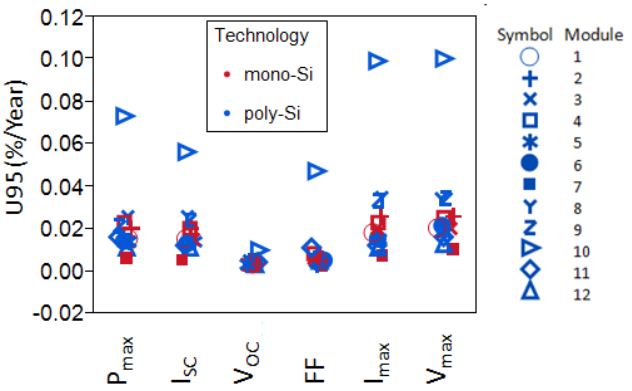

Fig. 10: Type A uncertainty for calculated degradation rates. Each module is represented by a different symbol. Mono-Si data are in red while poly-Si modules are in blue.

Poly-Si modules show a broader distribution of degradation rates than mono-Si modules, which could be an artifact due to most mono-Si modules coming from one manufacturer. The group of modules can be generally divided into two different categories: one is characterized by relatively modest decline in P_{max} of less than 0.5%/year (Modules 1-9), whereas the second group is characterized by P_{max} degradation significantly higher than 0.5%/year (Modules 10-12). The group with modest P_{max} degradation is characterized by large contributions due to I_{sc} degradation, which can more typically be attributed to delamination, discoloration, and cracked individual cells, while a smaller percentage can be attributed to light-induced degradation and soiling. [14, 15] The optical image of Fig. 11 shows two of these typical attributes: discoloration and soiling. The infrared (IR) image shows relatively uniform heating of the module and the absence of any hot-spot heating.

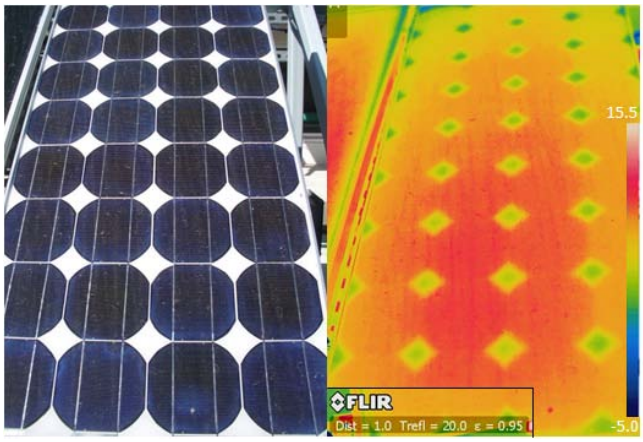

Fig. 11: Optical (left) and infrared (right) image of Module 7. Photo credit: Dirk Jordan, NREL PIX 20326.

In contrast, the group with the larger P_{max} degradation is characterized by large contributions due to FF degradation, indicating that series resistance may have increased or shunt resistance decreased. V_{oc} degradation is very low for both groups. Fig. 12 shows an overlay of temperature- and irradiance-corrected I-V curves from the beginning and end of life of Module 11, which display typical behavior of an increased series resistance during field exposure. The cause for Module 10 and 12 is not as clear and could be a combination of lowered shunt resistance, increased series resistance, or increased cell mismatch.

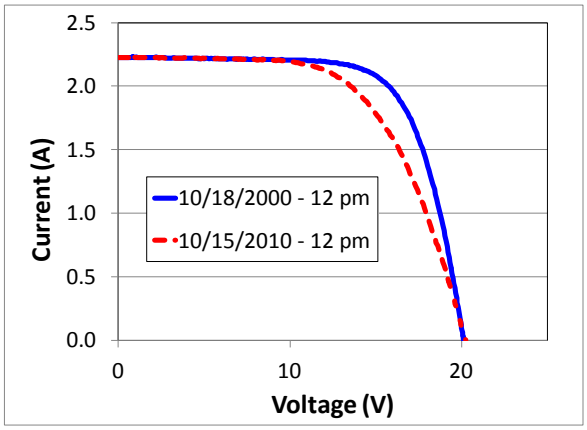

Fig. 12: Temperature- and irradiance-corrected I-V curves from the beginning of life (solid blue) and end of life (dashed red) of Module 11.

Lastly, an important question regarding inverter sizing is whether the P_{max} degradation is primarily due to current degradation or voltage degradation. In this study, 10 out of 12 modules showed < 0.2%/year degradation in V_{max}.

5. CONCLUSION

Twelve modules on the PERT at NREL were investigated for their long-term degradation in I-V parameters. For more accurate degradation rate determination, individual I-V curves were modeled, filtered, and then irradiance- and temperature-corrected. The majority of the modules showed < 0.5%/year degradation, with this degradation mostly linked to decreases in short-circuit current. Of the three modules that showed -0.6% to 1.1 %/year degradation, one showed clear evidence of increased series resistance with some degradation in current, while the other two showed a combination of causes.

6. ACKNOWLEDGMENTS

The authors would like to thank Joseph del Cueto for discussions about the PERT systems and Jose Rodriguez, Ed Gelak, and Carl Osterwald for PERT development and operations.

This work was supported by the U.S. Department of Energy under Contract No. DE-AC36-08-GO28308 with the National Renewable Energy Laboratory.

7. REFERENCES

(1) Jordan D.C., Kurtz S.R., Photovoltaic Degradation Rates – an Analytical Review, Progress in Photovoltaics: Research and Application, October 2011

(2) Skoczek, A., Sample, T., Dunlop, E.D., The Results of Performance Measurements of Field-aged Crystalline Silicon Photovoltaic Modules, Progress in Photovoltaics: Research and Application, 17, 227–240 (2009)

(3) Sanchez-Friera, P., Piliougine, M., Pelaez, J., Carretero, J., Sidrach de Cardona, M., Analysis of degradation mechanisms of crystalline silicon PV modules after 12 years of operation in Southern Europe, Progress in Photovoltaics: Research and Application (2011); DOI:10.1002/pip.1083

(4) Reis, A.M., Coleman N.T., Marshall M.W., Lehman P.A., Chamberlin, C.E., Comparison of PV module performance before and after 11-years of field exposure, IEEE PV Specialists Conference, New Orleans, LA, USA, 1432–1435 (2002)

(5) Chamberlin, C.E., Rocheleau, M.A., Marshall, M.W., Reis, A.M., Coleman, N.T., Lehman, P.A., Comparison of PV Module Performance Before and after 11 and 20 Years of Field Exposure, IEEE PV Specialists Conference, Seattle, WA, USA, (2011)

(6) Granata J.E., Boyson W.E., Kratochvil J.A., Quintana M.A., Long-Term Performance and Reliability Assessment of 8 PV Arrays at Sandia National Laboratories, Proceedings of the 34th IEEE PV Specialists Conference, Philadelphia, PA, USA, 1486–1491, (2009)

(7) del Cueto, J. A., Review of the Field Performance of One Cadmium Telluride Module, Progress in Photovoltaics: Research and Applicatio, 6, 433-446 (1998)

(8) ASTM standard E1036-08, Standard Test Methods for Electrical Performance of Nonconcentrator Terrestrial Photovoltaic Modules and Arrays Using Reference Cells, sections 8.5 through 8.10

(9) Emery, K.A., Osterwald, C.R., PV Performance Measurement Algorithms procedures, IEEE Photovoltaic Specialists Conference, Kissimmee, FL, USA, 1068-73 (1990)

(10) Standard Test Conditions (STC): Irradiance = 1000 W/m2, Tmodule = 25ºC

(11) Marion, B., Rummel, S., Anderberg, A., Current-Voltage Curve Translation by Bilinear Interpolation. Progress in Photovoltaics: Research and Applications, 12: 593–607 (2004)

(12) Anderson A.R., Photovoltaic Translation Equations: A New Approach, NREL report NREL/TP-411-20279, January 1996

(13) ISO Guide to the Expression of Uncertainty in Measurement or GUM, 1995. The U.S. edition of the GUM is entitled: American National Standard for Expressing Uncertainty--U.S. Guide to the Expression of Uncertainty in Measurement, ANSI/NCSL Z540-2-1997

(14) Quintana, M.A., King, D.L., Commonly observed degradation in field-aged PV modules, IEEE PVSC, New Orleans,1436 (2002)

(15) Sakamoto, S., Oshiro, T., Field Test Results on the Stability of c-Si PV Modules Manufactured in the 1990s, WCPEC, Osaka, Japan, 1888 (2003)